iBlink: A Wearable Device Facilitating Facial Paralysis Patients to Blink

Xiaohua Tian, *Member, IEEE*, Xuesheng Zheng, Yisheng Ji, Binyao Jiang, Tianyi Wang, Sijie Xiong, and Xinbing Wang, *Senior Member, IEEE*

Abstract—Facial paralysis makes patients lose their facial movements, which can incur eye damage even blindness since patients are incapable of blinking. We design and implement a pair of smart glasses *iBlink* to assist facial paralysis patients to blink. The basic idea is to monitor the normal side of the face with a camera and stimulate the paralyzed side, so that the blink of the both eyes become symmetric. Our contributions are: First, we propose an eye-blink detection mechanism based on support vector machine (SVM), which can detect asymmetric blinks of patients under various illumination conditions with an accuracy above 99 percent. Our eye-image library for training the model is published online for further related studies, which contains more than 30,000 eye images. Second, we design and implement an automatic stimulation circuits to generate electrical impulse for stimulating the patient's facial nerve branches, which can configure operational parameters in a self-adaptive manner for different patients. Third, we implement the entire *iBlink* system, which integrates the two functions above and a communication function module for tele-medicine applications. We conduct experiments in a hospital to obtain the design basis and verify effectiveness of our device.

Index Terms—Smart glasses, facial paralysis

1 Introduction

Facial paralysis is a disease making people losing facial movements, which is caused by nerve damages. People suffering from facial paralysis usually have muscles on one side of the face noticeably droop, which seriously impacts the person's quality of life. What is worse, facial paralysis can incur eye damage even blindness, because the eyelid on the affected side can not fully close, which makes the eye dry and infected by debris. The most common form of facial paralysis is known as Bell's palsy, which impacts 40,000 people in U.S. each year, where the typical symptom is the muscle dysfunction on one side of the face [1], [27].

Most Bell's palsy patients will completely recover in around 6 months with or without medical treatment; however, a few cases of facial paralysis patients could never completely return to normal. The current treatments for Bell's palsy include drugs and surgery, which are of side effect and controversial, respectively [1].

Efforts have been dedicated to find the cause of Bell's palsy; however, the exact cause is still unknown [1]. To the best of scientists' knowledge, the paralysis is due to the pressure incurred by infection in the tunnel containing main trunk of facial nerves, where the tunnel is inside of the people's head termed as *Facial canal*. An interesting phenomenon corroborating the theory is: using electric current of $3-11mA$ to stimulate the facial nerve branches could make the eye close for most of patients, which indicates that the facial muscle and nerve branches are still working.

In this paper, we propose to use wearable device to improve the facial paralysis patient's quality of life. In particular, we design and implement a pair of smart glasses *iBlink* to assist facial paralysis patients to blink. To the best of our knowledge, this is the first piece of wearable device for facial paralysis therapy. The basic idea of *iBlink* is to monitor the normal side of the face with a camera and stimulate the paralysed side, so that the blink of both sides of the face could become symmetric. As wearable devices such as Google glass are widely accepted, wearing *iBlink* could conceal the patient's defect and help them live like a normal people. Our contributions are as following:

First, we propose an eye-blink detection mechanism based on support vector machine (SVM), which can detect not only movements of eyes such as closing, opening and blink but also asymmetric blinks of facial paralysis patients under various lighting conditions (Section 4.2). We collected more than 30,000 eye images under different illumination conditions from 12 different people to train the SVM model. The detection accuracies are above 99 percent in ordinary lighting conditions. We publish the image library to support further related studies on facial paralysis [2].

Second, we design and implement an automatic stimulation circuit to generate electrical impulse for stimulating the user's facial nerve branches (Section 5). The circuit is controlled by a self-adaptive control mechanism, which accommodates individual and environment diversity. In particular,

- *X. Tian, Y. Ji, B. Jiang, T. Wang, S. Xiong, and X. Wang are with the School of Electronic Information and Electrical Engineering, Shanghai Jiao Tong University, Shanghai 200000, China. E-mail: {xtian, acetanil, emberspirit, tywang, qq420778733, xwang8}@sjtu.edu.cn.*
- *X. Zheng is with Xinhua Hospital, Shanghai Jiao Tong University School of Medicine, Shanghai 200240, China. E-mail: pheiphei@126.com.*

Manuscript received 11 Dec. 2017; revised 21 June 2018; accepted 30 Aug. 2018. Date of publication 3 Sept. 2018; date of current version 28 June 2019. (Corresponding author: Xiaohua Tian.)
For information on obtaining reprints of this article, please send e-mail to: reprints@ieee.org, and reference the Digital Object Identifier below.
Digital Object Identifier no. 10.1109/TMC.2018.2868660

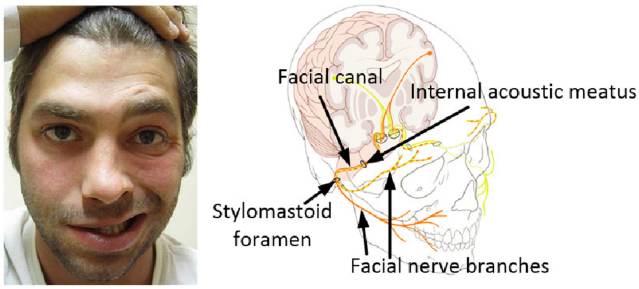

Fig. 1. Anatomy of facial nerves.

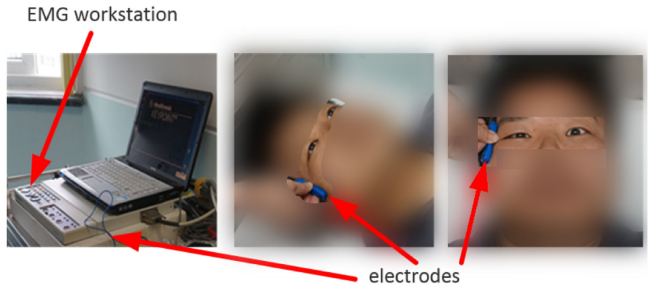

Fig. 2. Electrical stimulation induced blink.

the circuit can elevate stimulation level incrementally until an appropriate level is found for a specific user. We also implement a pain control protection scheme, so that the possible pain incurred by over stimulation can be avoided (Section 6.1); moreover, the circuit can also automatically switch to different levels to accommodate various users (Section 6.1). Further, we develop an approach to derive a person's blink frequency, so that the sampling frequency for anomaly detection can be adjusted for power saving (Section 6.2). Experiments show that the iBlink system could continuously work in the highest power consumption level for at least 10 hours with a lithium battery pack.

Third, we implement the *iBlink* prototype system, which integrates the mechanism mentioned above and a communication function module for tele-medicine applications (Section 7). The related computing and control mechanisms are hosted in a NanoPi S2 [32] platform, which connects other hardware components such as camera and stimulation circuits. We conduct experiments in a hospital with our device, which enables us to obtain the design basis of *iBlink* and verify the effectiveness of our device (Section 9.4).

2 Background and Motivation

Facial Paralysis. A person's facial muscles are controlled by facial nerves, and a facial paralysis sufferer has a dysfunction in the facial nerve system, thus loses the ability of facial movements. The left part of Fig. 1 shows a man with Bell's palsy on his right side of the face tries to raise his eyebrows and show his teeth [3]. It is clear that the facial muscles on his right side of face cannot move. The right part of Fig. 1 shows the anatomy of facial nerves based on [4]. The yellow and orange curves represent facial nerves of the left and right side of the face, respectively. The lesions typically occur at or beyond the stylomastoid foramen to the facial canal, which is a canal between the stylomastoid foramen and the internal acoustic meatus as shown in the right part of Fig. 1. Facial nerve branches are usually still working.

The basic aim of facial rehabilitation is facial symmetry at rest and when facial expressions are performed [21]. Eye protection plays a crucial role, since patients could not blink, which makes the eye lack of moisture and protection. The incurred complications such as corneal ulcer and lagophthalmos could further cause blindness. In clinical cases, doctors provide different treatments especially towards eye care based on an individual's expectation for recovery, degree of risk to the cornea and eye weakness [1], [9], [22].

Since a majority of Bell's palsy patients will completely recover in around 6 months, they normally take *supportive measures*, which include lubrication with artificial tears, ocular ointments and taping of the eyelid [30]. However, moisture chemicals has high risk of surface toxicity and tapes may touch the cornea or conjunctiva, which incur further trauma. *Static or dynamic surgical procedures* could be operated on prolonged and permanent paralysis sufferers. Nevertheless, such procedures involve complicated medical techniques and complications, which increase pain of patients [24], [28], [29], [31].

Electrical Stimulation. Transcutaneous electrical stimulation (TENS) is taken by physiotherapists as an option for enhancing recovery in patients with facial paralysis [6], [7], [10], which is to apply electrical stimulation to facial nerves without breaking the facial skin. The electrical stimulation has been proved safe and does not interfere with recovery [6], [11], [25].

An interesting observation of electrical stimulation is: the appropriate electrical stimulation could make people blink if the facial nerve branches are not damaged. We conduct an experiment in a hospital to verify the effect, as shown in Fig. 2. The device in the left sub-figure is a Medtronic Keypoint electromyography (EMG) workstation [8], which is used to evaluate and record the electrical activity produced by skeletal muscles. The EMG workstation can generate electric current impulses, which can be directed to the person's facial skin through a pair of electrodes as shown in the middle sub-figure. By appropriately configuring the strength, width and frequency of the impulse, the impulse can induce a person with functional facial nerve branches to blink as shown in the right sub-figure, where the right eye of the person is smaller than the left one as the right eye is to blink when the picture is taken.

Motivation. Our work in this paper is motivated by the electrical stimulation approach for facial paralysis treatment, and the observations of facial paralysis' characteristics. Since paralysis usually occurs in one side of the face and the facial nerve branches are usually functioning, we could use electrical stimulation to make the paralyzed side to move accordingly to make both sides of the face symmetric. In particular, the electrodes could be applied to nerve branches controlling blinks, so that the eye damage could be avoided. These functions could be implemented in a wearable smart glasses for the user's convenience, which could improve their quality of life before the paralysis goes away completely. Moreover, the electrical stimulation approach is non-invasive, thus the device could be considered as health care products as facemasks according to the FDA regulations [5], which avoids the all-consuming license application procedures for implanting devices.

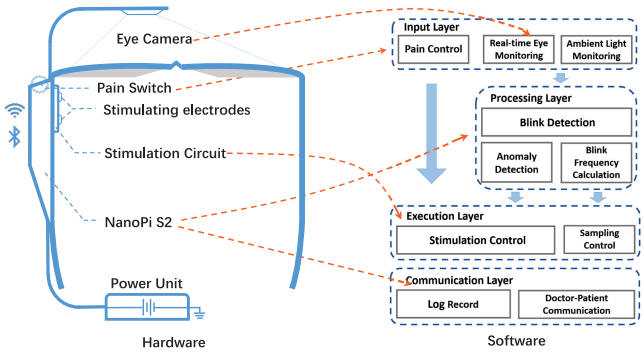

Fig. 3. Design of the iBlink system.

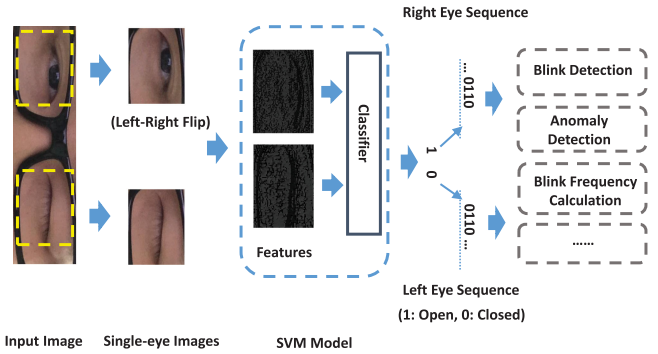

Fig. 4. Workflow of facial image processing.

3 Design and Challenges

The architecture design of *iBlink* is shown in Fig. 3, which includes hardware and software function modules.

Hardware. A camera is installed in front of the eyes to monitor blinks in real time. The eye camera captures images of both eyes and send them to the NanoPi S2 platform, which also monitors the ambient lighting condition. The NanoPi S2 and stimulation circuits are located on the patient's paralyzed side of the face. In particular, the NanoPi S2 and stimulation circuits are in the outer side of the glass frame, and two stimulating electrodes are in the inner side of the frame pressing on the patient's facial skin. The NanoPi S2 has Wi-Fi and Bluetooth interfaces which can be utilized for communication with smartphones. A power unit supports both the processing platform and the stimulation circuits. Our circuits also contain a potentiometer as the pain switch, which could fine-tune the automatic stimulation level control scheme. This is to accommodate individual diversity in case of discomfort.

Software. The software consists of four layers: input layer, processing layer, execution layer and communication layer. The input layer receives the input images and ambient illumination data from the camera and pain control action from the pain switch. The images and illumination data are sent to the processing layer for blink detection, anomaly detection and blink frequency calculation. The execution layer contains stimulation control and sampling control. The stimulation control takes in the result of detections and calculations from the processing layer to adjust the electric stimulation parameters for the patient automatically. It also responds to patients' actions on the pain switch. The sampling control takes in results from the processing layer and adjusts the sampling frequency of the camera. When a doctor needs to acquire the patient's pathology data or the patient needs to report the pathology records, they can transmit data via the communication layer. The communication layer can support both Wi-Fi and Bluetooth transmissions.

Challenges. First, the system has to accommodate individual diversity. The EMG clinical trials show that different patients require different configurations of the stimulation impulse to enable blinking. The blink frequencies of different people also vary, which makes efficient blinking detection difficult. Moreover, the paralysis could make muscles around the eye droop in different degrees for different patients, which also incurs difficulties for detecting asymmetric blinks.

Second, the system has to accommodate environment changing. The patient's current conditions are monitored by the camera, thus illumination conditions could significantly influence the accuracy of the detection layer; however, the illumination conditions could change due to people's mobility and time changing. Such an un-static factor also imposes the challenge to facial expression detection.

Third, the system has to be power efficient. This is the challenge for all mobile devices. In our case, we need to reduce the frequency of the power-consuming electrical impulses as much as possible. The stimulation circuit generates electrical impulses at the frequency of blink detection, while the camera has to monitor movements of the eyes at a high sampling rate to avoid information loss, which makes the sampling control a difficult trade-off and the power saving a noticeable challenge.

4 Facial Image Processing

4.1 Working Procedure

Facial image processing provides the basis of blink detection, anomaly detection and blink frequency calculation. The working procedure is shown in Fig. 4. The system needs to detect whether an eye is blinking. The event that the healthy eye is blinking and the other eye is not can be detected by the anomaly detection module, which initiates the stimulation circuits. By analyzing the sequence of blink detection, the system could estimate the patient's blink frequency, so that an appropriate sampling frequency for the camera could be obtained.

In particular, we use two fixed windows to cut the single-eye images from the camera input for each image frame captured by the eye camera. We train the support vector machine model with images of the left eye and the right-to-left flip of the right eye, so that we could use just one SVM model to detect status of two eyes. Using those sample images, we train the SVM model, where we particularly implement a classifier acting as a solver of the two-class classification problem, which labels 0 as eye closure and 1 as eye opening. A sequence of such labels could be used for detecting different events.

4.2 Support Vector Machine

The purpose of the image processing is to determine whether the eye is open or closed, which naturally can be modeled as a binary classification problem. We train a SVM model to obtain a classifier to realize the function.

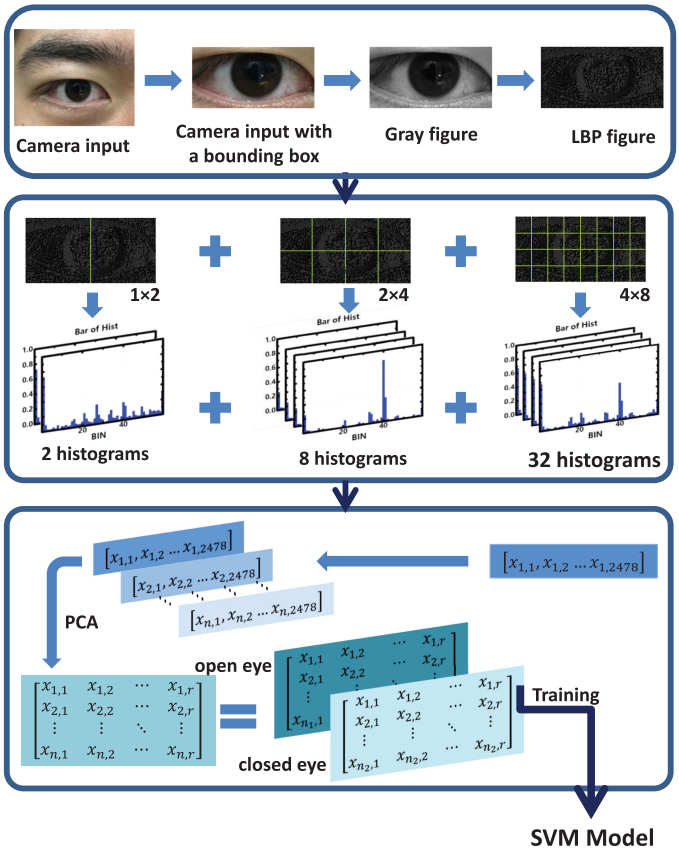

Fig. 5. Structure of pre-processing.

The method for training the SVM model is illustrated in Fig. 5. The camera captures the image of the patient's eye area as the input, which is then applied a bounding box so that the image only contains the eye. This is to minimize the noise from other facial regions in feature extraction. We here use Haar cascade classifier to detect the eye region and conduct adjustment to obtain the desired images. The remarkable feature of the eye-open or eye-close event is the proportion of the white part in the eye, where the black and white are dominant colors; therefore, we let the image with the bounding box be then processed to yield a gray figure, based on which an local binary pattern (LBP) figure can be obtained.

The LBP is another presentation of the image. In order to obtain the local binary pattern of the image, we compare each pixel with the 8 surrounding pixels to yield a 8-bit sequence. Each sequence is then converted into the decimal value, which is recorded as the value of the pixel's LBP in the image. The advantage LBP is its invariance to illumination conditions, which means that the model could work in different times of the day.

For each training sample image, we perform the processing as described above. We then divide the obtained LBP image into 1×2, 2×4 and 4×8 cells respectively. For each case, we could obtain a histogram for each cell as shown in the middle part of Fig. 5. The values of the pixels in the LBP are set into levels ranging from 0 to 58; the values along the horizontal axis of the histogram are from 0 to 58. The values along the vertical axis are the proportion of the pixels with corresponding values. The histogram for each cell can be regarded as an 1×59 vector. We then cascade the vectors for those cells and obtain an 1×2478 vector, because we will have $(1 \times 2 + 2 \times 4 + 4 \times 8) \times 59 = 2478$ values for each LBP image.

Considering that we have n sample images, we can obtain an $n \times 2478$ matrix, with combining all the 1×2478 vectors derived from the corresponding LBP images, as shown in the lower part of Fig. 5. We then perform the principal components analysis (PCA) to the matrix, which yields an $n \times r$ matrix. Suppose we have n_1 and n_2 sample images for the open-eye and closed-eye event respectively, then we can extract the sub-matrices derived from the open-eye and closed-eye sample images, which are used as inputs of the standard SVM training process. After that, we could obtain the SVM model for classifying the open-eye and closed-eye event.

In particular, we use the linear kernel function for the SVM training process and set the penalty factor C to be 1.0. Through experiments, we find that the linear kernel is much more suitable for this situation than Gaussian kernel. For each model, we use 67 percent of the images in the library for training, and the rest for verification, where we can observe the accuracy up to 99 percent in ordinary lighting situations.

4.3 Blink Detection and Anomaly Detection

After we have the eye status sequence, we define a blink sequence as a short status sequence in the form of '1,0,1', which means that the eye opens, then closes and opens again. Since a normal blink takes about 200 to 400 ms and our sampling rate is 20 to 30 frames per second, there could be multiple frames captured in a normal blink process. Multiple 1s and 0s can appear in a blink sequence, e.g., '1100011'. The adjustable sampling rate of iBlink ensures that there will be at least three consecutive 0s in a normal blink sequence. Since there could be false detection on the eye status, we introduce a polling method to correctly identify a blink action. For each detection, we take N_p sampling results in the eye status sequence in a sliding-window manner. If 0s are the majority in the poll, a blink will be identified. The polling method makes our system tolerant of detection exceptions in the eye status. The value of N_p is empirically set to 3 in our system.

The blink detection will be applied to both left and right eye sequences simultaneously. In most cases, people close and open their eyes at the same time, while a facial paralysis patient usually cannot close their eye on the ill-side. Consequently, if the blink detection process yields different results for two eye status sequences, we define it as an anomaly. Once an anomaly is detected, iBlink will give the patient an electrical stimulation through sending out a signal through GPIO interface of the NanoPi S2.

5 Stimulation Circuits

The stimulation circuits are consisted of a power adaption circuit, a power amplification circuit and a level control circuit, where how the circuits fit in the system is shown in Fig. 6. We use the lithium battery as the power source, which provides power supplies to both the computing platform and the execution circuits. The amplifying circuit takes in pulse width modulation (PWM) waves from the NanoPi S2 and amplifies the waves to generate the stimulation output on the stimulating electrodes. The level control circuit

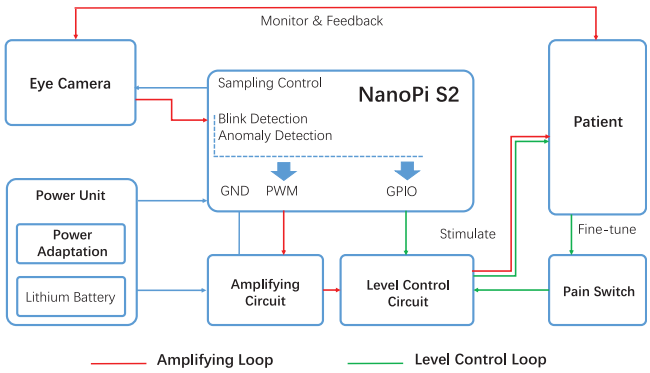

Fig. 6. Workflow of the stimulation module.

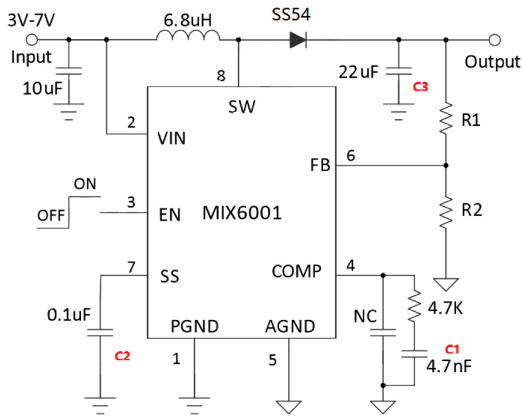

Fig. 7. Power adaption circuit diagram.

can adjust the power level the PWM waves are amplified, where the power level is assigned by the NanoPi S2 based on the patient's feedback. In this work, the level control circuit can maintain the stimulating power in 16 different levels. The working procedures of the circuits are denoted by loops in different colors as shown in Fig. 6.

5.1 Power Adaption Circuit

The power adaption circuit is to split the power source into two branches for the NanoPi S2 and the power amplification circuit, respectively. The circuit is essentially consisted of two DC-DC step-up circuits, where the circuit diagram is shown as in Fig. 7.

We use the DC-DC chip MIX6001 [33], where the output voltage is set by two feedback resistors R1 and R2. The internal feedback voltage of MIX6001 is 1.25V, and the output voltage is the product of the feedback voltage and a ratio of R1 + R2 to R2. For our specific scenario, we need to set R1 = $47k\Omega$, R2= $15k\Omega$ to generate a voltage of $5.16V$ for NanoPi, and set R1 = $47k\Omega$, R2= $5.2k\Omega$ to generate a voltage of $12.5V$ for the power amplification circuit. The circuit board is as shown in Fig. 8.

MIX6001 requires an inductor for energy storage, with which the function of voltage boosting can be realized. The datasheet of MIX6001 shows that the inductance value is supposed to be between $4.7\ \mu H$ and $10\ \mu H$. The less the DC resistance (DCR) of the inductor, the higher the efficiency of the step-up circuit. Moreover, the inductance has a rated working current parameter, which is normally related to the output power. In our case, the NanoPI needs 10W power, for which the rated current of the inductor should

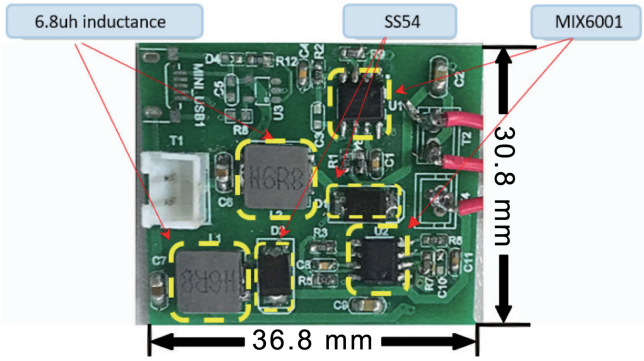

Fig. 8. Power adaption circuit implementation.

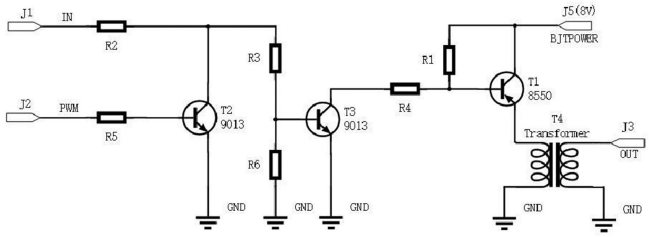

Fig. 9. Power amplification circuit diagram.

be at least 3.5A; therefore the corresponding inductance value can be set as $6.8\ \mu H$.

We use schottky diodes with high voltage resistance, high rated current and low forward voltage drop. The choice of the diode is closely related to the output current value. In this case, we choose a SS54 diode, which can satisfy the NanoPi's requirement of $2A$ current. Capacitor C1 and the resistor next to it together form the negative feedback on the input side and the compensation to the input. We choose to set the resistance and capacitance to be $4.7k\Omega$ and $4.7nF$, respectively. The capacitors C2 and C3 are used to prvent the alternating current (AC).

5.2 Power Amplification Circuit

The power amplification circuit takes in 3.7V PWM waves from the NanoPi and 12.5V power from the power adaption circuit, which are used to generate a much higher voltage to perform stimulation. In the amplifying loop denoted by the red line segments, the camera monitors blink actions of the patient; once an action of blink is detected, the NanoPi will send out the PWM wave, which is then boosted to the voltage between 100V and 200V. This is because the original voltage of the PWM wave is only 3.7V, which is far from enough to trigger a blink action. Due to the individual diversification, the specific stimulation voltage is adjusted by the level control circuit to be described in the next section.

The power amplification circuit diagram is shown in Fig. 9, where there are three bipolar junction transistors (BJTs), one transformer and several resistors. The port J1 (Lable: IN) and J2 (Lable: PWM) are used to take in the power supply and the PWM waves. We use 9013 NPN BJT triode [34] in the circuit, which is a kind of NPN low power triode mainly used for audio amplification and radio 1W push-pull output. The PWM wave is directed to T2's base to control the BJT's ON/OFF status: If the status is ON, T2's voltage is 0V and T3 will not be through, and the output port maintains the high level voltage for around 0.01 ms;

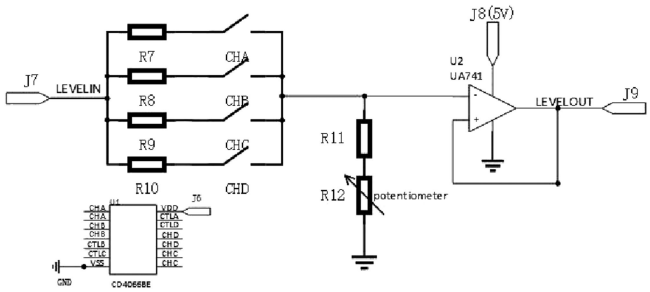

Fig. 10. Level control circuit.

otherwise, T3 will be through, then T1's emitter will stay at the low level voltage and control the output of the transformer. The type of the PNP BJT T1 is 8550 [35], which is characterized by small signal, low voltage and high current. This kind of BJTs are mainly used in switches and RF amplification. The transformer escalates the voltage of PWM waves to about 100V output. Although the instantaneous voltage is very high, the stimulation is safe since the high voltage lasts only for about 0.01 ms. The lithium battery pack provides 7.4V power supply to the circuit by Port J5 (to T1,s emitter and R1), and a pair of finely placed stimulating electrodes which are connected to the output from Transformer are used to stimulate the patient's facial nerve branches.

For the stimulating electrodes, we use electrodes made of conductive ointment, which can be finely attached to human skin and have good electrical conductivity. The distance between the two stimulating electrodes is set to be 3.3 cm, which is chosen empirically from our experiments and clinical trials to invoke the best stimulation reactions. Those conductive ointment electrodes can be easily changed for maintenance purpose on a regular basis. The implementation of the amplifying circuit is shown in the left part of Fig. 11.

5.3 Level Control Circuit

The level control circuit takes in the GPIO signals and the fine-tuning pain switch input to adjust the level of the stimulation, as shown in the level control loop of Fig. 6. The level control circuit diagram is shown in Fig. 10. It can be seen that the circuit consists of a bilateral switch chip CD4066BE [36], an operational amplifier chip UA741 [37] and a potentiometer. The switch CD4066BE has 4 channels that are essentially 4 switches, and the switches are corresponding to 4 control ports: CTLA, CTLB, CTLC and CTLD as shown in Fig. 10. When a control port gets high level voltage, the switch will be turned on so that the current could pass through the corresponding channel; otherwise, the channel will not be through. The bilateral switch chip takes in GPIO control signals from the NanoPi and changes the output voltage level of the stimulating electrodes by switching the state of the four switches in CD4066BE chip.

However, the channel is not an ideal wire, which in fact has a resistance of about 150 to 200Ω, thus we actually design the level control circuit based on a parallel circuit. In our experiment, the channel resistance is about 200Ω; we set R7 = 0Ω, R8 = 150Ω, R9 = 450Ω and R10 = 1050Ω, so that the resistances of the 4 channels are maintained as CHA = 150Ω, CHB = 300Ω, CHC = 600Ω and CHD = 1200Ω. This is to enable the entire parallel circuit to switch among 16 different resistance values. In the GPIO control signal, '0' means low level voltage signal and '1' means high level voltage signal, CD4066BE obtains control signal from NanoPi like "1011" to change the parallel circuit's resistance. We also use a potentiometer as a pain switch to allow the patient to adjust the output voltage manually. The potentiometer is designed to adjust the voltage only within one stimulation level in case of misoperation, its maximum resistance is $1k\Omega$ and we add R11 to set the resistance range to be between 1500Ω and 1150Ω. As an example, if we set the value of R12 to be 600Ω, the relationship among control signal, resistance value and the corresponding output voltage is as shown in Table 1, where Vin is the input voltage from port J7. Note that J7 is actually connected with the output port J3 of the power amplification circuit as shown in Fig. 9. The operational amplifier chip UA741 is used as a voltage follower to isolate the effect caused by level control circuit's resistance to amplifying circuit. The level control circuit is shown in the right part of Fig. 11.

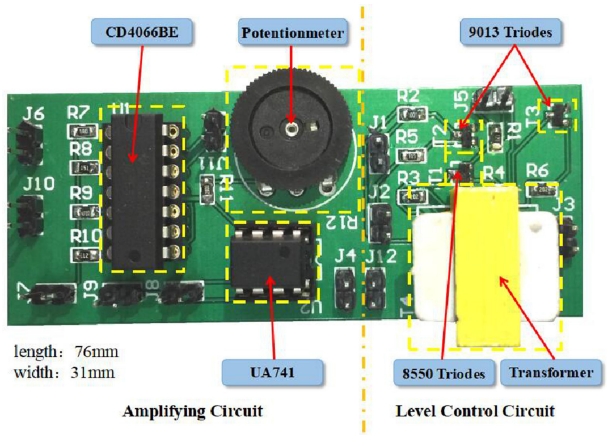

Fig. 11. Power ampliation and level control circuit implementation.

TABLE 1
Some Examples of Output Voltage

Signal	Resistance (Ω)	Output Voltage
0011	100	$6/7Vin$
0101	120	$5/6Vin$
0001	150	$4/5Vin$
0110	200	$3/4Vin$
0010	300	$2/3Vin$
0100	600	$1/2Vin$
1,000	1,200	$1/3Vin$

Due to unpredictable factors such as temperature, humidity and shape of human skin, conductivity of the skin varies not only among different people but also in different time and places. It is impossible to accurately set the stimulation intensity to a fixed value; our level control circuit provides both automatic stimulation level selection and manual fine-tuning capabilities.

6 Automatic Control Mechanism

6.1 Stimulation Control

Requirements Analysis. First, the conductivity of human skin varies in different situations as mentioned in the previous section, thus the stimulation thresholds for different

TABLE 2
Measurement of Critical Points on Different People

Label	Gender	Age	Critical Point (mA)
1	Female	42	5.7
2	Male	19	10.6
3	Male	35	7.0
4	Male	28	6.4
5	Female	22	4.5

individuals also vary. We conduct clinical experiments on 5 volunteers in a hospital with the EMG workstation. The equipment we use in the hospital measures the stimulation intensity by electric current. Table 2 shows the critical points for stimulation reactions of different patients. The values of the electric current thresholds are found by manually increasing the value by a step-size of 0.1 mA, which is inconvenient and inefficient. There is a need of a mechanism that can automatically and efficiently find patients' critical points of stimulation.

Second, patients wear the iBlink on a daily basis, where the electric stimulations are applied to the patients according to the result of real-time image processing. Since the status of a human body and the surrounding environment can be changing in different times of a day, dynamically adjusting the stimulation parameters is a practical need.

Third, since human facial skin is very sensitive, in case of discomfort or pain, the iBlink needs to adjust the stimulation parameters in time according to the real-time feedback from the patients. Thus, automatic stimulation control is a must for our medical device.

Mechanism Design and Implementation. We define four working modes for the iBlink system:

- *Startup Mode:* When the patient wears the device for the first time and turns on the system, the iBlink automatically searches for a lowest stimulation level that can invoke an eye-closing reaction. The corresponding stimulation voltage is recorded for future use.
- *Daytime Mode:* The iBlink works in this mode when the illumination condition is good. This is the basic mode that runs in majority time of a day.
- *Nighttime Mode:* When the illumination intensity is low, iBlink works in this mode.
- *Pain Control Mode:* This mode runs concurrently with the other four modes. Once receives the patient's signal, the iBlink automatically decreases the stimulation level to avoid pain by over stimulating.

Fig. 12 shows the workflow of the automatic stimulation control, where ALI means ambient light intensity and T_p is the pain threshold. The automatic stimulation control mechanism relies mainly on the input of illumination data and blink detection results. In the startup mode, the stimulation level starts from 0 and increases incrementally. The eye camera monitors the feedback of the patient's eyes. If there is no blink resulting from the stimulation, the stimulation level continues to rise, until it reaches the level that causes an eye-closing reaction. The eye camera also monitors the illumination data, with which a model selector can switch between daytime mode and nighttime mode. Then the image processing module will choose SVM models trained

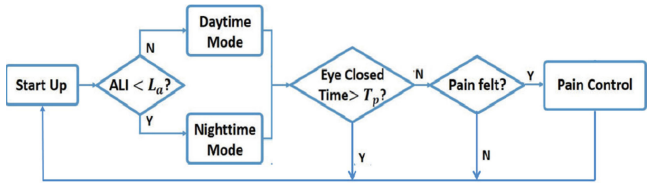

Fig. 12. Working flow of automatic control mechanism.

under different lighting conditions to perform blink detection. In case of discomfort or pain, which means there exists an over stimulating situation, the patient can give a signal by closing the healthy-side eye for a certain length of time. This triggers the pain control mode and the stimulation level starts dropping, until a new critical level is found. The pain control algorithm is shown in Algorithm 1.

Algorithm 1. Pain Control Algorithm

Require: Control Threshold $\mathbf{C_T}$;Test times $\mathbf{k}$;
Minimum Level $\mathbf{Level_{min}}$;
Initial Level $\mathbf{Level_{init}}$;
Ensure: Level series changing with time **Level**[]
$\mathbf{k} \leftarrow 1$, $\mathbf{Level}[\mathbf{k}] \leftarrow \mathbf{Level_{init}}$
$\mathbf{t_1} \leftarrow getSystemTime()$, $\mathbf{s_1} \leftarrow getEyeStatus()$
while True **do**
  $\mathbf{k} \leftarrow \mathbf{k} + 1$
  $\mathbf{t_2} \leftarrow getSystemTime()$, $\mathbf{s_2} \leftarrow getEyeStatus()$
  if $\mathbf{s_2}$ = Open **then**
    $\mathbf{s_1} \leftarrow \mathbf{s_2}$
    $\mathbf{Level}[\mathbf{k}] \leftarrow \mathbf{Level}[\mathbf{k}-\mathbf{1}]$
  else
    if $\mathbf{s_1}$ = Open **then**
      $\mathbf{t_1} \leftarrow \mathbf{t_2}$
      $\mathbf{s_1} \leftarrow Closed$
      $\mathbf{Level}[\mathbf{k}] \leftarrow \mathbf{Level}[\mathbf{k}-\mathbf{1}]$
    else
      if $\mathbf{t_2} - \mathbf{t_1} > \mathbf{C_T}$ **then**
        $\mathbf{t_1} \leftarrow \mathbf{t_2}$
        $\mathbf{Level}[\mathbf{k}] \leftarrow \mathbf{Level}[\mathbf{k}-\mathbf{1}] - 1$
        if $\mathbf{Level}[\mathbf{k}] < \mathbf{Level_{min}}$ **then**
          $\mathbf{Level}[\mathbf{k}] \leftarrow \mathbf{Level_{min}}$
        end if
      end if
    end if
  end if
end while

6.2 Sampling Control

Normally, people can keep their eyes open for about 2 seconds to 8 seconds and then close their eyes for about 0.2 seconds to 0.4 seconds. To capture the exact movement of patients' eyes, the camera sampling frequency should be neither too low to lose useful information nor too high to consume much power. In this section, we describe our adaptive sampling algorithm which automatically adjusts the system's sampling frequency.

Upper and Lower Bounds of Sampling Interval. We set the upper bound of sampling interval B_U to be 0.05 seconds, which ensures there will be at least 3 eye-closing images captured by the camera. Since the fastest sampling frequency of our camera is 30 Hz, the lower bound of the sampling interval B_L is 0.033 seconds.

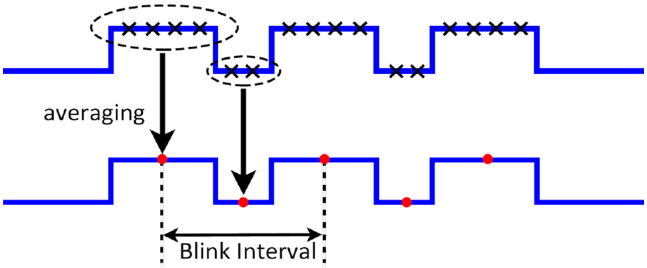

Fig. 13. Definition of the blink interval.

Adaptive Sampling Algorithm. Suppose the sampling interval is τ_s, it can be expressed as

$$\tau_s = B_L + (B_U - B_L)r, \tag{1}$$

where r is a factor with $0 < r < 1$. We calculate the blink interval τ_b by averaging the time of all neighboring points of the same status in the blink graph and aggregate them into one point. The blink graph is derived by applying the polling method to the eye status sequences during blink detection. In this way, all neighboring points on blink graph are of different status. The blink interval is the time interval between two neighboring points when the eye is open. The definition of the blink interval is defined in Fig. 13.

It is worth noting that there are two parameters M and α in the adaptive sampling algorithm for automatically adjusting the camera sampling frequency. We use M to calculate the average period of single blink and use α to determine how to adjust the sampling frequency. When we are calculating the current time-interval, we look back to the past $M \cdot 2$ sampling intervals, where M is a predefined positive integer. We calculate the average of the early M blink intervals as $\bar{\tau_b^1}$ and the average of the other M intervals as $\bar{\tau_b^2}$. We set a empirical threshold τ_T and compare $\bar{\tau_b^1}$ with $\bar{\tau_b^2}$. Different events can be defined according to the comparison result:

- Advance Event: $\bar{\tau_b^2} - \bar{\tau_b^1} > \tau_T$, i.e., the increment of blink interval is larger than the threshold.
- Back-off Event: $\bar{\tau_b^1} - \bar{\tau_b^2} > \tau_T$, i.e., the decrement of blink interval is larger than the threshold.
- Stable Event: $|\bar{\tau_b^1} - \bar{\tau_b^2}| < \tau_T$, i.e., the change of blink interval is within the threshold.

If the Advance Event is detected, the iBlink increases the sampling frequency as the patient has the tendency to increase their blink frequency. If the Back-off Event is detected, the iBlink decreases the sampling frequency.

The new r under Advance Event can be calculated as

$$r = \hat{r} - \alpha_D \hat{r}, \tag{2}$$

where $0 < \alpha_D < 1$, $\hat{r}$ is the previous r and α_D is a constant factor controlling the rate at which r decreases.

The new r under Back-off Event can be calculated as

$$r = \hat{r} + \alpha_I(1 - \hat{r}), \tag{3}$$

where $0 < \alpha_I < 1$ and α_I is a constant factor controlling the rate at which r decreases.

The design of the formula makes r decrease slower and increase faster when it is small and increase slower and decrease faster when it is big. The parameter r will change the sampling interval accordingly. We set the initial value of r to be 0.5, which is empirically suitable for most of patients. The adaptive sampling algorithm is shown in Algorithm 2.

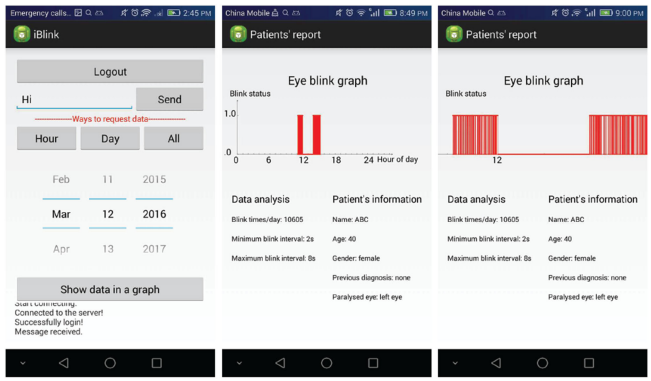

Fig. 14. (a) Data request page. (b) Data analysis page. (c) Data analysis page (Zoomed in).

Algorithm 2. Adaptive Sampling Algorithm

Require: Lower bound of sampling interval $\mathbf{B_L}$;
Upper bound of sampling interval $\mathbf{B_U}$;
Parameter of sampling interval $\mathbf{r}$;
Increasing factor $\alpha_\mathbf{I}$; Decreasing factor $\alpha_\mathbf{D}$;
Turn count $\mathbf{t}$; Average window $\mathbf{M}$.
Ensure: All sample time $\mathbf{S}[]$;

$\mathbf{t} \leftarrow 1, \mathbf{r} \leftarrow 0.5$
$\tau_\mathbf{s} \leftarrow \mathbf{B_L} + (\mathbf{B_U} - \mathbf{B_L})\mathbf{r}$
$\mathbf{S[0]} \leftarrow 0, \mathbf{S[t]} \leftarrow \mathbf{S[t-1]} + \tau_\mathbf{s}$
while True **do**
  if $\mathbf{t}$ $geq 2 \cdot M$ **then**
    $\tau_\mathbf{s}^1 \leftarrow 0, \tau_\mathbf{s}^2 \leftarrow 0$
    for $i = 0 \rightarrow M$ **do**
      $\tau_\mathbf{s}^1 \leftarrow \tau_\mathbf{s}^1 + S[t - 2M + i] - S[t - 2M + i - 1]$
      $\tau_\mathbf{s}^2 \leftarrow \tau_\mathbf{s}^2 + S[t - M + i] - S[t - M + i - 1]$
    end for
    $\tau_\mathbf{s}^1 \leftarrow \tau_\mathbf{s}^1/M, \tau_\mathbf{s}^2 \leftarrow \tau_\mathbf{s}^2/M$
    if $\tau_\mathbf{s}^2 - \tau_\mathbf{s}^1 > \tau_T$ **then**
      $\mathbf{r} \leftarrow \mathbf{r} - \alpha_\mathbf{D}\mathbf{r}$
    else if $\tau_\mathbf{s}^1 - \tau_\mathbf{s}^2 > \tau_T$ **then**
      $\mathbf{r} \leftarrow \mathbf{r} + \alpha_\mathbf{I}(1 - \mathbf{r})$
    end if
  end if
  $\tau_\mathbf{s} \leftarrow \mathbf{B_L} + (\mathbf{B_U} - \mathbf{B_L})\mathbf{r}$
  $\mathbf{t} \leftarrow \mathbf{t} + 1$
  $\mathbf{S[t]} \leftarrow \mathbf{S[t-1]} + \tau_\mathbf{s}$
end while

7 Communication between the Patient and the Doctor

We develop an APP to enable the iBlink system to be linked to the smart phone. The APP could collect and analyze data of the patients and send the derived information to the doctor. The doctor can request different analyzed data from the patients' devices. The communication module leverages the Wi-Fi interface of NanoPi S2. The screenshots of the APP is shown in Fig. 14, from left to right is the data request page, data analysis page and its zoomed in view.

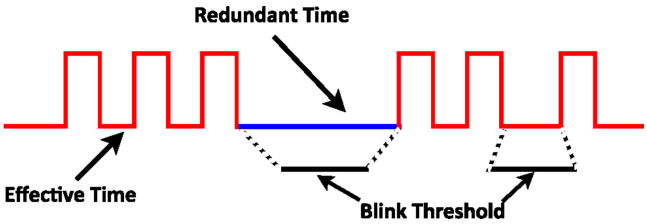

Fig. 15. Effective time selection.

TABLE 3
Components of the System

Component	Properties
NanoPi S2	CPU: S5P4418, dynamic frequency from 400 Mhz to 1.4 GHz
Eye Camera	640×480, 30fps
CD4066BE	$-0.5V$ to $20V$, $\pm 10\ mA$
9,013 triode	NPN, $I_{max} = 0.5A$, $625\ mW$
8,550 triode	PNP, $I_{max} = 0.5A$, $625\ mW$

The three buttons on the data request page stand for three ways to transmit data. The "Hour" button starts a thread to request all the current day's saved data from the patient, stores them in a file and append newly collected data to the file every hour. The "Day" button will request the previous day's data and save them in a file. The "All" button will request all the data on the server and save them in files identified by date.

The data analysis page shows the blink data in a blink graph and gives data analysis result, e.g., blink times per day, minimum blink interval and maximum blink interval. The data are recorded to help doctors to better study the patients' pathology features.

Since sometimes intervals of blinks can be useless, like when the eye is closed due to sleep or rest for a long time, we devise a way to detect effective time interval during a day. If any time interval between two blinks is longer than a predefined value, that interval will be discarded and not be stored in the record. The process is illustrated in Fig. 15. The predefined value is empirically chosen to be 10 seconds.

8 System Implementation

The components of the system are tabulated in Table 3. Fig. 16a shows the main components of the iBlink smart glasses. The iBlink prototype is consisted of a NanoPi S2 platform, stimulation execution circuits, a pair of stimulating electrodes, an eye camera and a power unit. We use NanoPi S2 as the main processor. We design our own stimulation circuits with amplifying and level control circuit embedded. The pain switch is implemented by a potentiometer to fine-tune the voltage output on the stimulating electrodes. For wearing comfort and convenience, we design our own spectacles frame using 3D printing. The components can easily be attached to the designed spectacles frame. Fig. 16b shows our wearable prototype.

9 Performance Evaluation

9.1 Eye Status Detection

We first show the LBP feature maps for eye images with different status and illumination conditions, and then evaluate

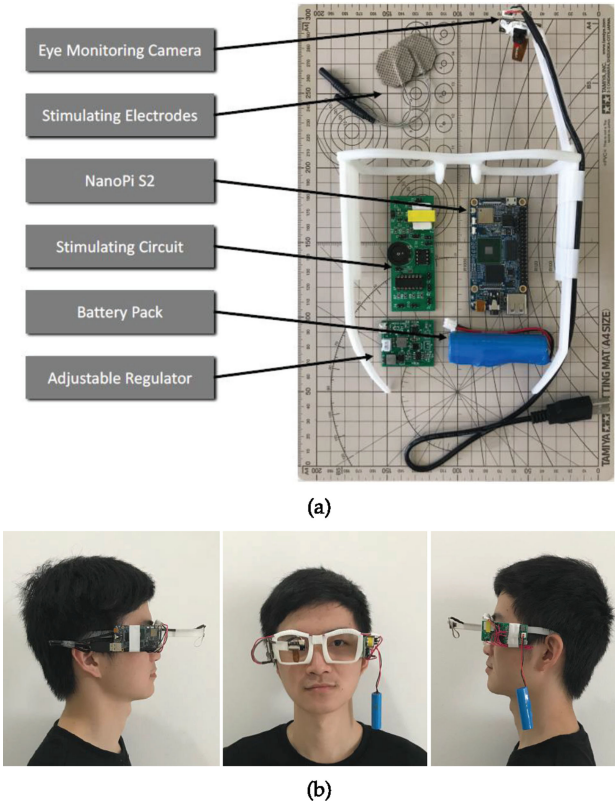

Fig. 16. (a) The main components of iBlink. (b) The wearable prototype.

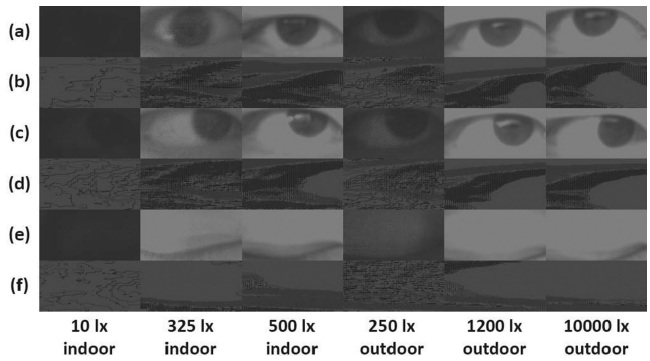

Fig. 17. Eye images and feature maps after the uniform lbp transform.

performance of eye status detection by measuring the accuracy of the proposed SVM model.

Fig. 17 shows open and closed eye images under different illumination conditions and the LBP feature maps for the image. Row (a) and row (c) show the open eye images in different scenarios, and row (b) and row (d) contain the feature maps after LBP transformation. The closed eye images and the corresponding feature maps are shown in row (e) and row (f). The six columns demonstrate 6 different scenarios under different illumination conditions. The average illumination intensities from left to right are: $10lx$, $325lx$, $500lx$ (in the laboratory), $250lx$, $1200lx$ and more than $1500lx$ (in the outdoor spaces), respectively. The illumination intensities correspond to six major scenarios a patient will encounter in daily life. Basically, column 1-3 represent the indoor scenarios under different lighting conditions, including the nighttime scenario, indoor on a cloudy day with dim light, and indoor on a sunny day with affluent

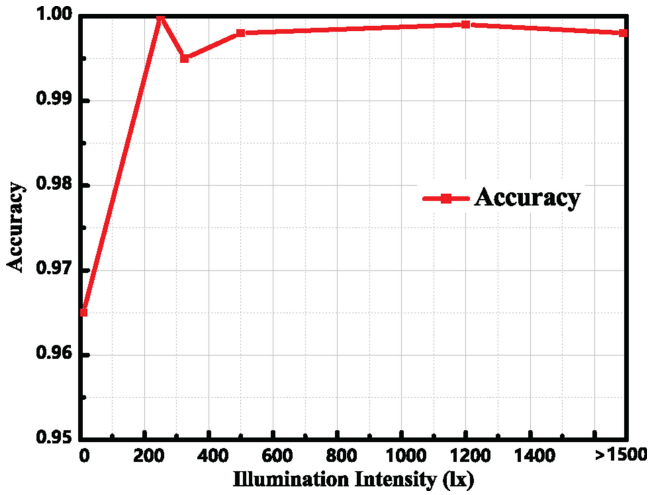

Fig. 18. Eye status detection.

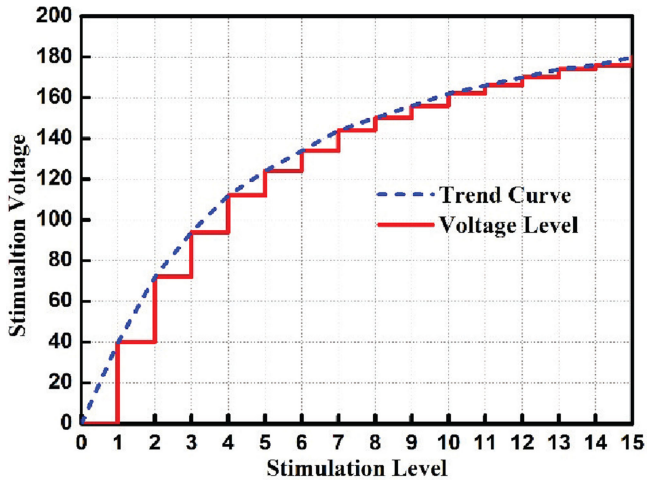

Fig. 19. Voltage - Stimulation level.

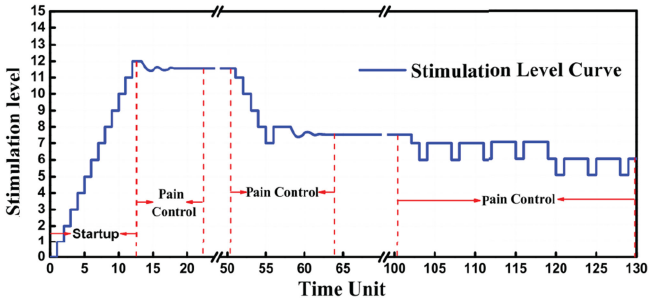

Fig. 20. The change of stimulation level.

sunlight; column 4-6 demonstrate three typical outdoor scenarios, in the shadow of buildings, outdoor on a cloudy day and outdoor with sufficient sunlight.

In Fig. 17, the feature maps of open-eye images in row (b) and row (d) all have triangle dark areas in the middle, which actually represent the eyeball, while in row (f) the closed eye is indicated by line segments in the feature maps. Note that values of the closed-eye images' feature maps in column 1 are high and difficult to discern, which can result in low accuracy in the classification step. This is caused by low illumination intensity.

The eye status detection accuracy of our proposed SVM model is shown in Fig. 18. We randomly select images of 5 subjects for each illumination condition in the data library. With the illumination intensity over $100lx$, the model's accuracy is very close to 100 percent. When the illumination condition reaches more than $1500lx$, the accuracy slightly drops due to the existence of some extreme cases, i.e., the illumination intensity reaches more than $10000lx$. Since those extreme cases are rare and unlikely to happen, our daytime model satisfies patients' needs in daily use scenarios.

9.2 Automatic Stimulation Control

According to the clinical trial, a voltage between $100V$ to $200V$ can trigger an eye-closing reaction. We divide the output voltage into 16 levels in our circuits, ranging from 0 to 184V. Fig. 19 shows the output voltage for each stimulation level and the trend curve of the levels. We design the increment of each level to the previous level in a non-uniformly manner, where the increment becomes smaller as the level rises. This is because we need those levels with high voltages to increase slowly in case of discomfort or pain, and those with low voltages to increase fast to reach the critical point.

To test our stimulation control method in practice, we record the change of stimulation level by measuring the output voltage of the stimulating electrodes. Fig. 20 shows the output stimulation level change we recorded. Our test covers all the scenarios we considered in the stimulation control. The startup phase is from time unit 0 to 12. The stimulation level continues to rise according to the feedback from the eye camera. When it reaches the lowest level that can cause an eye-closing reaction, i.e., a critical point, the rising procedure stops and the voltage stabilizes on that stimulation level. Starting from time unit 13 to 18 is the first pain control phase. It is when the patient feels a mild pain and needs to fine-tune the voltage output. Note that fine-tuning can increase or decrease the voltage in at most half range of the current stimulation level. The stimulation level eventually stabilizes on a voltage that is slightly smaller than the voltage of level 12.

At the 50th time unit the second pain control starts. In this phase, the patient feels a relatively strong pain and triggers the close-eye method. When iBlink detects the patient closes his eye for more than 3 seconds, the stimulation level starts dropping and stops at the first level that cannot invoke the eye-closing reaction. Then the level rises back by one to the new critical level that can cause the eye-closing reaction. The patient then fine-tunes the voltage by the pain switch. After time unit 100, the patient simulates falling asleep. The close-eye method is again triggered. The stimulation control attempts to drop the stimulation level every several time units. When the attempted stimulation level causes an eye-closing reaction, the voltage stabilizes at the lower level. By this method, the stimulation level is always kept on the lowest level that can trigger an eye-closing action.

9.3 Power Consumption

Power consumption is the crux of wearable devices, which also applies to iBlink. We use a 7.4V lithium battery pack as the power unit to do the power consumption experiment, which provides power supply for both blink detection and stimulation subsystems. A natural question to ask is: how long the battery pack could support operations of the entire system. To answer this question, we conduct power

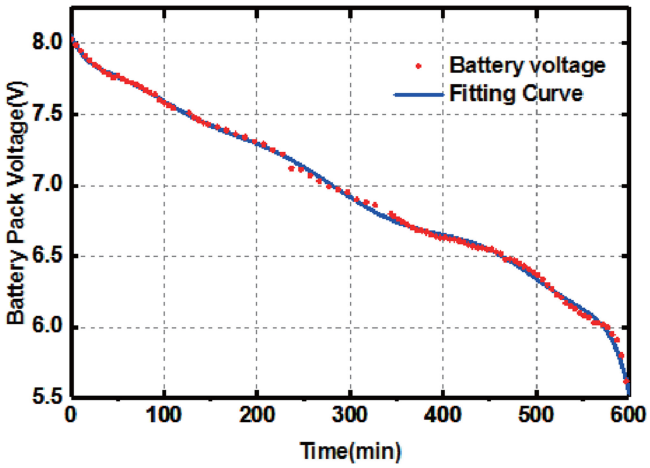

Fig. 21. Power consumption.

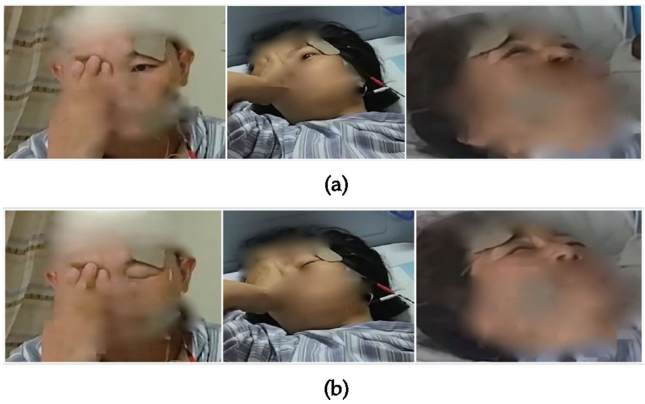

Fig. 22. (a) Before stimulation. (b) After stimulation.

consumption experiments and measure the voltage of the battery pack during the device's usage. In the experiment process, we activate the blink detection mechanisms all the time and set the highest stimulation level for the stimulation circuits. The voltage of the battery pack is measured every 10 minutes. The purpose of such a setting is to make the system operate in the highest power consumption level so that the worst case scenario can be examined. The experimental results are shown in Fig. 21, which presents how the voltage of the battery pack changes as the time goes on. It indicates that the 7.4V lithium battery pack can support the system's operation in the worst power consumption scenario for at least 10 hours, which is sufficient for a patient's daytime use.

9.4 Experiments on Volunteers

We conduct experiments on volunteers in a hospital to verify the function of our system under the doctor's supervision. There are six volunteers testing the stimulation circuits. We illustrate the testing snapshots of some of the patients with their permissions in Figs. 22 and 23. In the process as shown in Fig. 22, the doctor sticks the brown ointment electrodes to the facial nerve branches near the abnormal eye as shown in Fig. 22a. We increase the stimulation level gradually to manually simulate the Startup Mode until the eye is stimulated to close as shown in Fig. 22b. Table 4 shows the critical level for stimulation of corresponding patients. All of the six patients report no feeling of pain during the whole test and only the 43-aged female

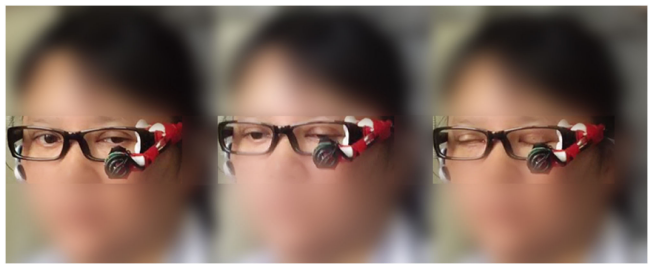

Fig. 23. Experiment on Volunteers.

TABLE 4
Critical Stimulation Levels of Different Patients

Label	Gender	Age	Critical stimulation level
1	Male	21	12
2	Male	22	13
3	Female	30	7
4	Male	35	7
5	Female	43	9
6	Female	59	11

volunteer mentions a slight sense of tingling. All volunteer patients appreciate our work and believe the product is useful for facial paralysis patients.

Another middle-aged female patient volunteers to try our prototype as shown in Fig. 23. The left image in Fig. 23 is the patient's normal eye status. The camera is installed on the healthy left side of face and the electrodes are on the right side of her face, which is paralyzed. We can see that her right eye opens a little wider than the healthy side eye. The middle image is when the patient is closing her left eye while her right eye cannot be closed. This is when the iBlink sends out the stimulation signals. The right image in Fig. 23 shows the situation when the electric stimulation invokes an eye-closing reaction and the patient is able to close both of her eyes. The result of this trial proves that our device can satisfy the patient's requirement.

10 Related Work

Kim et al. propose to use smart phones to diagnose facial paralysis [26], where the 'asymmetric index' is proposed to evaluate the degree of asymmetry of both sides of the face. Through measuring the asymmetric index during different expressions like resting, eye-brow raising and smiling, the smartphone could help determine if the facial paralysis happens to the person. However, the diagnosis accuracy reaches only 89 percent, which still needs significant improvement. In contrast to the work that just proposes an approach to facilitate diagnosis of facial paralysis, we design and implement a wearable device to provide eye protection for paralysis patients.

Wearable computing devices such as Google glasses have been attracting much attention in recent years. Efforts have been dedicated to not only design and implement new types of glasses with interesting functions, but also utilize existing equipment to carry out jobs like data collection and analysis. *iGaze* [19] and *iShadow* [18] are representatives of smart glasses proposed recently. *iGaze* establishes person-to-person as well as person-objects communication by

recognizing eye gaze action. Mayberry et al. propose *iShadow*, where the power consumption of real-time sensing is dramatically reduced. Rallapalli et al. realize physical analysis in retail stores based on customer behaviors collected from smart glasses. Although smart glasses are prevailing nowadays, most existing devices just focus on entertainment. Our work in this paper focuses on eye protection for facial paralysis patients, which is an urgent requirements for a special group of people.

11 Conclusion

We have designed and implemented iBlink, a pair of smart glasses to provide eye protection for facial paralysis patients. We have proposed an eye-movements detection mechanism based on SVM, which can detect asymmetric eye-movements of patients under various illumination conditions. Our library for training SVM models has been published online for further related studies. Moreover, we have designed and implemented an automatic stimulation circuits to generate electrical impulse for the patient's facial nerve branches stimulation, which can configure operational parameters in a self-adaptive manner for different patients. Further, we have implemented the entire *iBlink* system, which integrates the two functions above and a communication function module for tele-medicine applications. We have conducted comprehensive clinical trials in a hospital, in order to obtain the design basis and verify effectiveness of our device.

Acknowledgments

The work in this paper is supported by the National Key Research and Development Program of China 2017YFB1003000, and National Natural Science Foundation of China (No. 61872233, 61572319, 61829201, 61532012, 61325012, 61428205). A preliminary version of this article appears in the *Proceedings of The 15th ACM International Conference on Mobile Systems, Applications and Services* (*ACM MobiSys 2017*).

References

[1] National institute of neurological disorders and stroke, "Bell's palsy fact sheet," 2018. [Online]. Available: http://www.ninds.nih.gov/disorders/bells/detail_bells.htm
[2] Eye image library. 2016. [Online]. Available: https://www.dropbox.com/s/vgrk4mfkpjmc0jo/EyeData.zip?dl=0
[3] Picture of a Bell's palsy patient from wikepedia. 2018. [Online]. Available: https://en.wikipedia.org/wiki/Bell%27s_palsy#/media/File:Bellspalsy.JPG
[4] Figure of anatomy of facial nerves. 2018. [Online]. Available: https://en.wikipedia.org/wiki/Stylomastoid_foramen#/media/File:Facial_canal.png
[5] FDA regulations on facemasks. 2018. [Online]. Available: http://www.fda.gov/MedicalDevices/ProductsandMedicalProcedures/GeneralHospitalDevicesandSupplies/PersonalProtectiveEquipment/ucm055977.htm
[6] P. Alakram and T. Puckree, "Effects of electrical stimulation in early Bell's palsy on facial disability index scores," *SA J. Physiotherapy*, vol. 67, no. 2, pp. 35–40, 2011.
[7] S. M. Sandeep and V. N. Jayprakash, "Effect of electrical stimulation on facial grading system in subjects with early facial palsy," *Nat. J. Integr. Res. Med.*, vol. 4, pp. 29–32, 2013.
[8] Electromyography. 2018. [Online]. Available: https://en.wikipedia.org/wiki/Electromyography
[9] J. Cole, S. Zimmerman, and S. Gerson, "Nonsurgical neuromuscular rehabilitation of facial muscle paresis," *Rubin LR (ed): The Paralyzed Face*, vol. 24, no. 2, pp. 107–122, 1991.
[10] D. J. Farragher, "Electrical stimulation: A method of treatment for facial paralysis," *Rose FC, Jones R, Vrbova G (eds): Neuromuscular Stimulation: Basic Concepts Clinical Implications.*, vol. 3, pp. 303–306, 1989.
[11] C. S. Cohan and S. B. Kater, "Suppression of neurite elongation and growth cone motility by electrical activity," *Sci.*, vol. 232, pp. 1638–1640, 1986.
[12] M. C. Brown and R. L. Holland, "A central role for denervated tissues in causing nerve sprouting," *Nature*, vol. 282, pp. 724–726, 1979.
[13] D. Prutchi and M. Norris, *Design and Development of Medical Electronic Instrumentation: A Practical Perspective of the Design, Construction, and Test of Medical Devices*. Hoboken, NJ, USA: Wiley, 2005
[14] Y. Jia, E. Shelhamer, J. Donahue, S. Karayev, J. Long, R. Girshick, S. Guadarrama, and T. Darrell, "Caffe: Convolutional architecture for fast feature embedding," in *Proc. ACM Int. Conf. Multimedia*, 2014, pp. 675–678.
[15] V. Nair and G. E. Hinton, "Rectified linear units improve restricted boltzmann machines," in *Proc. 27th Int. Conf. Mach. Learn.*, 2010, pp. 807–814.
[16] G. E. Hinton, N. Srivastava, A. Krizhevsky, I. Sutskever, and R. R. Salakhutdinov, "Improving neural networks by preventing co-adaptation of feature detectors," Available: https://arxiv.org/pdf/1207.0580.pdf
[17] A. Krizhevsky, I. Sutskever, and G. E. Hinton, "ImageNet classification with deep convolutional neural networks," in *Proc. 25th Int. Conf. Neural Inf. Process. Syst.*, 2012, pp. 1097–1105.
[18] A. Mayberry, P. Hu, B. Marlin, C. Salthouse, and D. Ganesan, "iShadow: Design of a wearable, real-time mobile gaze tracker," in *Proc. 12th Annu. Int. Conf. Mobile Syst. Appl. Serv.*, 2014, pp. 82–94.
[19] L. Zhang, X. Li, W. Huang, K. Liu, S. Zong, X. Jian, P. Feng, T. Jung, and Y. Liu, "It starts with igaze: Visual attention driven networking with smart glasses," in *Proc. 20th Annu. Int. Conf. Mobile Comput. Netw.*, 2014, pp. 91–102.
[20] Z. Zhu and Q. Ji, "Robust real-time eye detection and tracking under variable lighting conditions and various face orientations," *Comput. Vis. Image Understanding*, vol. 98, no. 1, pp. 124–154, 2005.
[21] I. Mavrikakis, "Facial nerve palsy: Anatomy, etiology, evaluation, and management," *Orbit*, vol. 27, no. 6, pp. 466–474, 2008.
[22] U. S. Rao, J. Poll, and M. T. Yen, "Prognosis for recovery vital to facial nerve palsy management," *Ophthalmology Times*, vol. 34, no. 19, pp. 24–26, 2009.
[23] S. L. Spruance, "Bell palsy and herpes simplex virus," *Ann. Internal Med.*, vol. 120, no. 12, 1994, Art. no. 1045.
[24] A. K. Das, K. Sabarigirish, and R. C. Kashyap, "Facial nerve paralysis: A three year retrospective study," *Indian J. Otolaryngology Head Neck Surg.*, vol. 58, no. 3, pp. 225–228, 2006.
[25] P. Alakram and T. Puckree, "Effects of electrical stimulation on house-brackmann scores in early bells palsy," *Physiotherapy Theory Practice*, vol. 26, no. 3, pp. 160–166, 2010.
[26] H. Kim, S. Kim, Y. Kim, and K. Park, "A smartphone-based automatic diagnosis system for facial nerve palsy," *Sensors*, vol. 15, no. 10, pp. 26756–26768, 2015.
[27] H. Kim, S. Kim, Y. Kim, and K. Park, "What is Bell's palsy?" *Harvard Women's Health Watch*, vol. 8, no. 10, 2001, Art. no. 8.
[28] V. Gelder, S. Ronald, and L. Gelder, "Facial expression and speech: Neuroanatomical considerations," *Int. J. Psychology*, vol. 25, no. 10, pp. 141–155, 1990.
[29] H. Arion, "Dynamic closure of the lids in paralysis of the orbicularis muscle," *Plastic Reconstructive Surg.*, vol. 50, no. 6, 1972, Art. no. 629.
[30] D. Moral-Fatio and J. Laiardrie, "Palliative surgical treatment of facial paralysis. The palpebral spring," *Plastic Reconstructive Surg.*, vol. 33, no. 5, pp. 446–456, 1964.
[31] F. Masters, D. Robinson, and J. Simons, "Temporalis transfer for lagopthalmos due to seventh nerve palsy," *The Amer. J. Surg.*, vol. 110, no. 4, pp. 607–611, 1965.
[32] NanoPi S2. 2016. [Online]. Available: http://wiki.friendlyarm.com/wiki/index.php/NanoPi_S2
[33] Datasheet of MIX6001. 2016. [Online]. Available: https://www.datasheeticpdf.com/index.php?route=product/search&search=MIX6001
[34] Datasheet of 9013. 2016. [Online]. Available: http://datasheet.eeworld.com.cn/pdf/WINGS/66397_9013.pdf
[35] Datasheet of 8550. 2016. [Online]. Available: http://datasheet.eeworld.com.cn/pdf/142482_STANSON_8550.html
[36] Datasheet of CD4066BE. 2016. [Online]. Available: http://www.ti.com/lit/ds/symlink/cd4066b-mil.pdf
[37] Datasheet of UA741. 2016. [Online]. Available: http://www.ti.com.cn/cn/lit/ds/symlink/ua741.pdf

Xiaohua Tian (S'07-M'11) received the BE and ME degrees in communication engineering from Northwestern Polytechnical University, Xian, China, in 2003 and 2006, respectively, and the PhD degree from the Department of Electrical and Computer Engineering (ECE), Illinois Institute of Technology (IIT), Chicago, in Dec. 2010. Since Mar. 2011, he has been with the School of Electronic Information and Electrical Engineering, Shanghai Jiao Tong University, and now is an associate professor with the title of SMC-B scholar. He serves as the column editor of the *IEEE Network Magazine* and the guest editor of the *International Journal of Sensor Networks* (2012). He also serves as the TPC member for IEEE INFOCOM 2014-2017, best demo/poster award committee member of IEEE INFOCOM 2014, TPC co-chair for IEEE ICCC 2014-2016, TPC co-chair for the 9th International Conference on Wireless Algorithms, Systems and Applications (WASA 2014), TPC member for IEEE GLOBECOM 2011-2016, and TPC member for IEEE ICC 2013-2016, respectively. He is a member of the IEEE.

Xuesheng Zheng received the MD degree from Zhejiang University, in 2006. From 2006 to 2009, he was trained at the first affiliated Hospital of Zhejiang University School of Medicine, and then promoted to attending physician. Since 2010, he has been working with the Department of Neurosurgery, Xinhua Hospital affiliated to Shanghai Jiaotong University School of Medicine, and has served as deputy chief physician since 2013. His main research field is the surgical treatment of cranial nerve diseases, including facial paralysis, hemifacial spasm and trigeminal neuralgia. He has published more than 20 SCI papers.

Yisheng Ji received the BS degree in electrical engineering from Shanghai Jiao Tong University, Shanghai, China, in 2018. He is currently working toward the MS degree in computer engineering at the University of California, San Diego, California. From 2016 to 2018, he was a research assistant with the Research Center of Intelligent Internet of Things, Shanghai Jiao Tong University, China. His research interests include computer vision and image processing, wearable devices and mobile computing.

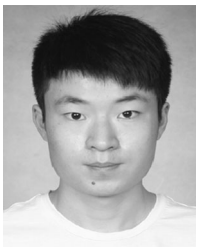

Binyao Jiang is currently working toward the BE degree in computer science from Shanghai Jiao Tong University, China and is expected to graduate in 2019. His recent research work is on indoor localization.

Tianyi Wang received the BSc degree in electronic engineering from the School of Electronic Information and Electrical Engineering, Shanghai Jiao Tong University. He is currently working toward the master's degree at Shanghai Jiao Tong University. His research interests include circuit design, embedded development, pattern recognition, and image reconstruction.

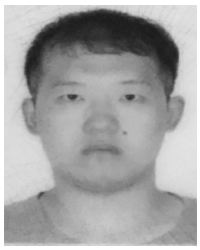

Sijie Xiong received the BE degree in information engineering from Shanghai Jiao Tong University, in 2017. His recent research interests include mobile network and system.

Xinbing Wang received the BS degree (with hons.) from the Department of Automation, Shanghai Jiaotong University, Shanghai, China, in 1998, the MS degree from the Department of Computer Science and Technology, Tsinghua University, Beijing, China, in 2001and the PhD degree, major in the Department of electrical and Computer Engineering, minor in the Department of Mathematics, North Carolina State University, Raleigh, in 2006. Currently, he is a professor with the Department of Electronic Engineering, Shanghai Jiaotong University, Shanghai, China. He has been an associate editor for the *IEEE/ACM Transactions on Networking* and the *IEEE Transactions on Mobile Computing*, and the member of the Technical Program Committees of several conferences including ACM MobiCom 2012, ACM MobiHoc 2012-2014, IEEE INFOCOM 2009-2017. He is a senior member of the IEEE.